Jahn-Teller transition in TiF_3 investigated using density-functional theory

Vasili Perebeinos* and Tom Vogt
Department of Physics, Brookhaven National Laboratory, Upton, New York 1973-5000, USA
(Received 28 April 2003; revised manuscript received 9 September 2003; published 8 March 2004)

We use first-principles density-functional theory to calculate the electronic and magnetic properties of TiF_3 using the full-potential-linearized augmented-plane-wave method. The local density approximation (LDA) predicts a fully saturated ferromagnetic metal and finds degenerate energy minima for high- and low-symmetry structures. The experimentally observed Jahn-Teller phase transition at $T_c = 370$ K cannot be driven by the electron-phonon interaction alone, which is usually described accurately by the LDA. Electron correlations beyond the LDA are essential to lift the degeneracy of the singly occupied Ti t_{2g} orbital. Although the on-site Coulomb correlations are important, the direction of the t_{2g}-level splitting is determined by dipole-dipole interactions. The LDA+U functional predicts an aniferromagnetic insulator with an orbitally ordered ground state. The input parameters $U = 8.1$ eV and $J = 0.9$ eV for the Ti $3d$ orbital were found by varying the total charge on the TiF_6^{2-} ion using the molecular NRLMOL code. We estimate the Heisenberg exchange constant for spin 1/2 on a cubic lattice to be approximately 24 K. The symmetry lowering energy in LDA+U is about 900 K per TiF_3 formula unit.

DOI: 10.1103/PhysRevB.69.115102 PACS number(s): 71.15.Mb, 62.20.−x, 71.30.+h, 64.60.−i

I. INTRODUCTION

There is an ongoing interest in phase transitions in perovskite-based materials. Above $T_c \approx 370$ K the trifluoride TiF_3 has the cubic framework perovskite structure AMX_3, with no A cations present. Each Ti is at the center of a corner sharing fluorine octahedra MX_6. At low temperatures the structure becomes rhombohedral. This symmetry lowering can to a first approximation be characterized by a titling of the rigid MX_6 octahedra about the threefold axis. The nominal valance of the titanium ion is $3+$, with one $3d$ electron occupying the triply degenerate t_{2g} orbital in the high-temperature phase. One may expect a Jahn-Teller instability in TiF_3. Indeed in the distorted structure titanium has a D_{3d} local environment, in which the t_{2g} orbitals are split into an a_{1g} and a doublet e_g orbital. The trigonal distortions have been intensively discussed in the context of other t_{2g} compounds, like FeO (Ref. 1) and $LaTiO_3$ (Ref. 2).

We use density-functional theory (DFT) to investigate the cubic to rhombohedral structural phase transition which has been established by x-ray diffraction.[3,4] Many trifluoride MF_3 compounds (M = Al, Cr, Fe, Ga, In, Ti, V) exhibit this structural phase transition.[3–6] It is believed that the observed transition in TiF_3 is of a ferroelastic nature.[3] In most of those materials except for TiF_3 and MnF_3 there are no partly filled d shells. The driving mechanism for the ferroelastic transitions can be pictured as the formation of dipole moments on fluorine atoms due to the asymmetric distribution of the $2p$ electron density in the distorted structure. The long-range dipole-dipole interaction favors a distorted structure with antipolar arrangement of dipoles.[7] The local density approximation (LDA) captures both the long- and short-range interactions on the same footing and predicts a distorted structure to have a minimum energy in AlF_3.[8]

In the present studies we choose the TiF_3 system with a partly filed t_{2g} shell. The Jahn-Teller energy lowering due to the lifting of the t_{2g} orbital degeneracy in the distorted structure should add up to the long-range dipole formation energy. Unexpectedly, we find the total energies of the high- and low-temperature phases to be identical within the errors of calculations. The failure of the LDA to explain this phase transition is due to the fact that transition-metal d electrons are not adequately described by the LDA. Although the dipole-dipole long-range interaction favors the distorted structure, however, the electron kinetic energy of the t_{2g} one-third-filled band is increased due the diminishing of the hopping integral (t) between neighboring Ti atoms due to octahedra tilting. The two effects mutually cancel each other, resulting in degenerate minima of the potential energy surface.

It was realized some time ago that the LDA tends to underestimate the Coulomb repulsion of electrons occupying different orbitals of the same d shell.[9] In particular, this leads to equal occupations of different orbitals of the same manifold and prevents stabilization of the orbitally ordered solutions. The LDA+U functional, however, generates an orbital-dependent potential which favors solutions with broken orbital degeneracy. LDA+U calculations indicate that the low-temperature phase has a by about 900 K lower energy per TiF_3 than the high-temperature phase. One of the roles of the Coulomb interaction is to suppresses the electron kinetic energy of the partly filled t_{2g} bands. The bandwidth narrowing in the distorted structure effectively reduces the restoring force to rotate the octahedra which facilitate stabilization of the distorted structure. The electronic ground state is orbitally ordered in the low-temperature phase with one electron occupying the a_g orbital oriented along the rhombohedral direction forming a Heisenberg spin-1/2 lattice coupled antiferromagnetically to its neighbors via a superexchange mechanism.

In this work we use the molecular NRLMOL code[10] to calculate U by varying the occupation number of the Ti d orbital of the TiF_6^{2-} ion. These calculations are significantly less computationally demanding compared to the supercell approaches,[9,11,12] and since only the first neighboring fluo-

 ©2004 The American Physical Society

rines mostly contribute to the screening, a good estimate for parameters U and J can be readily achieved in the calculations.

The Hund interaction and electron kinetic energy are realistically described with the LDA. The TiF_3 compound is predicted to be a ferromagnetic metal with a fully saturated magnetic moment of $1\mu_B$ per formula unit. The exchange Hund energy is large and the Stoner criterium is satisfied. The electron-phonon interaction lifts the on-site degeneracy of the t_{2g} orbitals and for a sufficiently strong coupling a gap in the spectrum can open. We estimate the electron-phonon coupling (≈ 2 meV/deg) to be insignificant to open the gap and to drive the phase transition in TiF_3. Although the on-site Coulomb correlations are important, the direction of the t_{2g}-level splitting is determined by the long-range dipole-dipole interaction.[7] Many successes and failures of the LDA in transition-metal oxide compounds have been summarized, for example, in the review article in Ref. 13.

II. METHOD OF CALCULATION

The purpose of this paper is to elucidate the electronic structure of TiF_3 and explain the structural phase transition using the DFT method. This is done using the full-potential-linearized augmented-plane-wave (FP-LAPW) method[14] with local orbital extensions[15] in the WIEN2k implementation.[16] The LDA Perdew-Wang[17] exchange-correlation potential was used. Well-converged basis sets and Brillouin zone sampling were employed. The crystal structure was reported by Kennedy and Vogt.[4] It is cubic at high temperature with a unit cell volume 58.8 ($Å^3$). A rhombohedrally distorted structure of the space group $R3c$ can be characterized by three parameters: (1) volume 56.5 ($Å^3$), (2) the octahedra tilt $\phi = 13°$, and (3) a $c/a = 1.0315$ ratio, which measures the distortion along the rhombohedral direction. There are two titanium and six fluorine atoms in the rhombohedral unit cell. The fluorine ions are sitting in the $6e$ sites $[(x, -x+1/2, 1/4)$,etc.], and $\delta = x - 0.75$ is the deviation from cubic positions. The octahedra tilting angle is related to δ by $\tan(\phi) = 2\sqrt{2}\delta$. The calculations for *both* the high- and low-symmetry phases were performed using two formula units per unit cell and the same k-point mesh, with 292 special k points in the irreducible Brillouin zone. A tetrahedron method was used for integration over the Brillouin zone.

III. LDA RESULTS

We first calculate the cubic phase by fixing $\phi = 0$ and $c/a = 1$ in the rhombohedral structure of the space group $R3c$. The LDA finds a ferromagnetic ground-state solution with a fully saturated magnetic moment of $1\mu_B$ per Ti. The volume optimization is shown in Fig. 1. The equilibrium volume $V_0 = 58.6$ $Å^3$ is in excellent agreement with the experiment.[4] The bulk modulus of 111 GPa is extracted by fitting a Murnaghan[18] equation of state. The c/a ratio was fixed to the experimental value 1.0315 at $T = 10$ K and the two parameters are relaxed to find the minimum of the low-symmetry structure. The energy minimization with respect to the volume for the fixed $c/a = 1.0315$ and $\phi = 10°$ is shown in Fig. 1 and yields $V_m = 56.2$ $Å^3$.

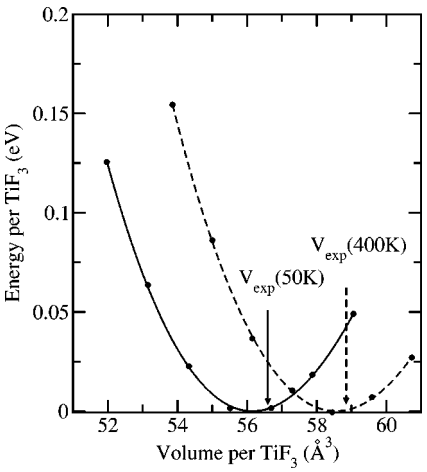

FIG. 1. Calculated total energy of ferromagnetic high-T phase ($\phi = 0$, $c/a = 1$—dashed line) and low-T phase ($\phi = 10°$, $c/a = 1.0315$—solid line) as a function of volume.

Further optimization with respect to the tilt angle for a fixed minimum volume V_m and the same c/a ratio did not significantly alter the ground-state energy. The optimal tilt angle is $\phi_0 = 10.5°$. The Ti-F bond is the most rigid bond in the structure, and therefore it is convenient to plot the energy versus the Ti-F bond length. A parabola fit to the energy variation shown in Fig. 2 is excellent and yields a spring constant of the single bond $K = 13.9$ eV/Å. The Ti-F bond length d in the $R3c$ crystal structure is

$$d^2 = a_h^2[1/12 + \delta^2 + (c/a)^2/24], \tag{1}$$

where $a_h = a\sqrt{2}$ is the hexagonal a lattice constant. Knowing the spring constant for the bond stretching and equilibrium volume V_0 the bulk modules can be estimated as $B = K/(6V^{1/3}) \approx 96$ GPa.

The total energy differences of the high- and low-T phases are beyond the accuracy of calculations. Despite the

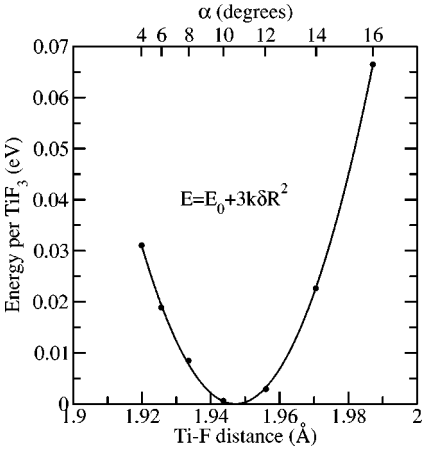

FIG. 2. Calculated total energy of the ferromagnetic low-T phase as a function of tilt angle and fixed volume (V_m) and $c/a = 1.0315$ ratio. The optimal Ti-F distance is 1.947 Å and the spring constant is 13.9 eV/$Å^2$.

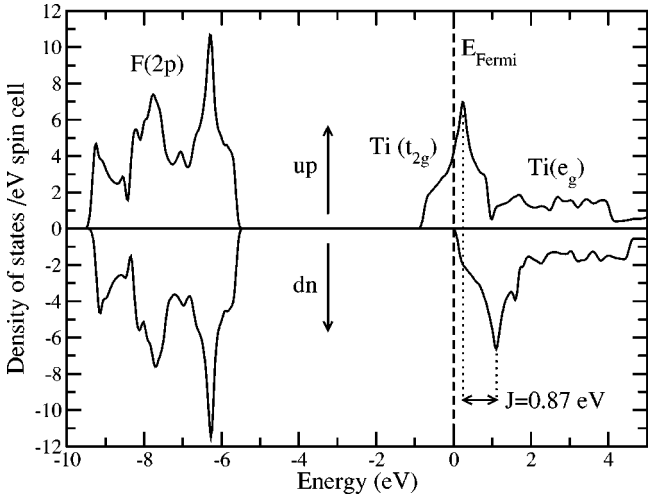

FIG. 3. Density of states of the ferromagnetic solution for the high-T phase. The t_{2g} and e_g bands are split by the crystal field energy ≈ 2 eV. The t_{2g} bandwidth is about 2 eV, which corresponds to hopping parameter $t=0.25$ eV. The Hund coupling $J=0.87$ eV can be estimated from the relative position of the spin-up and spin-down peak positions.

excellent agreement with the experimental structural parameters, the LDA total energy analysis does not explain the high temperature of the observed structural phase transition.

The densities of states are shown in Fig. 3. The t_{2g} band lies at the Fermi level and it is one-third filled. The Hund energy dominates the kinetic energy such that the Stoner criterion is satisfied and the material becomes magnetic. The band structure of the Ti t_{2g} electrons can easily be understood with a nearest-neighbor two-center Slater-Koster[20] model. The orbitals $|\alpha\beta\rangle$ have hopping matrix elements with themselves along the α and β directions with amplitude $t=(dd\pi)$. The tight-binding fit in the high-temperature phase with $t=0.25$ eV is shown in Fig. 4.

In the low-temperature phase the Ti-F-Ti bond angle is smaller than 180°, which reduces the hopping and narrows the bandwidth. The on-site orbital degeneracy is lifted by the octahedron tilting. In the D_{3d} local Ti site symmetry the t_{2g} manifold splits into

$$a_g=\frac{|xy\rangle+|yz\rangle+|zx\rangle}{\sqrt{3}},$$

$$e_{g1}=\frac{|yz\rangle-|zx\rangle}{\sqrt{2}},$$

$$e_{g2}=\frac{2|xy\rangle-|yz\rangle-|zx\rangle}{\sqrt{6}}. \tag{2}$$

The bandwidth in the tilted structure $\phi=\phi_0$ corresponds to reduced $t=0.225$ eV and the electron-phonon Jahn-Teller energy gap at the Γ point is 6 meV. From the simple tight-binding model with these parameters the kinetic energy loss due to the band narrowing effect is 18 meV and it is not even compensated by the lifting of the orbital degeneracy. The total LDA energy includes the lattice and electronic degrees of freedom and predicts degenerate minima within the errors of calculations (Fig. 1). The LDA failure to predict the cubic-to-rhombohedral phase transition can be rationalized by the lack of electron correlation effects in the LDA method.

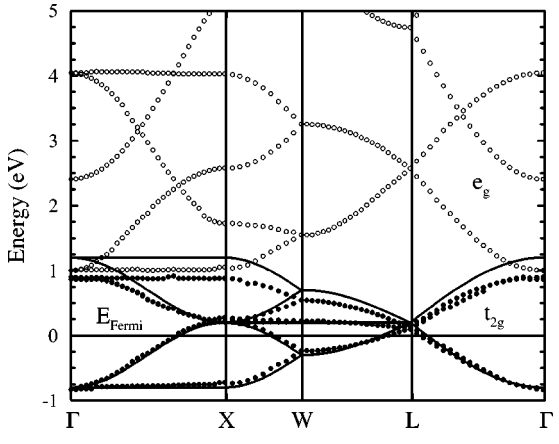

FIG. 4. Calculated band structure along the high-symmetry line in the high-symmetry structure: e_g bands, open circles; t_{2g} bands, solid circles. The solid line is a tight-binding fit, which uses a single Slater-Koster parameter $t=(dd\pi)=0.25$ eV. The Fermi level is at zero energy.

IV. PARAMETER $U(J)$ CALCULATION FOR THE LDA+U METHOD

In extending the LDA method to account for correlations resulting from on-site interactions Anisimov, Zaanen, and Andersen[9] (AZA) chose to refine LDA by including an orbital-dependent one-electron potential to account explicitly for the important Coulomb repulsions not treated adequately in the LDA approach. This was accomplished in accordance with Hartree-Fock theory by correcting the mean-field contribution of the d-d on-site interaction with an intra-atomic correction. This correction has been applied in slightly different ways. We use the SIC LDA+U functional[19] as implemented in the WIEN2k package.

In this work we use a single TiF_6^{2-} ion to calculate the parameters U and J. In these calculations the screening due to the nearest-neighboring fluorines is taken into account and there are no other Ti atoms for the d electron to hop to. The TiF_6^{2-} ion forms an octahedra with a Ti-F bond of 1.93 Å with the Ti atom placed in the center. The total energy and d orbital chemical potential of the TiF_6 can be modeled by the single-site Hubbard model:

$$E=E_0-\varepsilon(n_\uparrow+n_\downarrow)+\frac{U}{2}(n_\uparrow+n_\downarrow)^2-\frac{J}{2}(n_\uparrow^2+n_\downarrow^2),$$

$$\mu_\uparrow=\frac{\partial E}{\partial n_\uparrow}=-\varepsilon+U(n_\uparrow+n_\downarrow)-Jn_\uparrow, \tag{3}$$

where $n_\uparrow$ and $n_\downarrow$ are occupation numbers of the triply degenerate t_{2g} molecular orbital. We use two sets of self-consistent calculations to determine the parameters U and J. The quadratic total energy and linear chemical potential fits to the

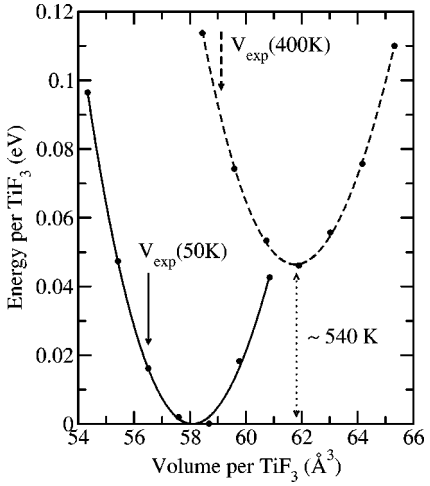

FIG. 5. LDA+U calculations of the antiferromagnetic high-T phase ($\phi=0°$, $c/a=1$—dashed line) and low-T phase ($\phi=12°$, $c/a=1.0315$—solid line) as a function of the volume of TiF_3. Coulomb and exchange parameters were chosen as $U=8.1$ eV and $J=0.9$ eV. The optimal volumes of 61.8 Å^3 and 58.1 Å^3 agree well with experimental results indicated by arrows.

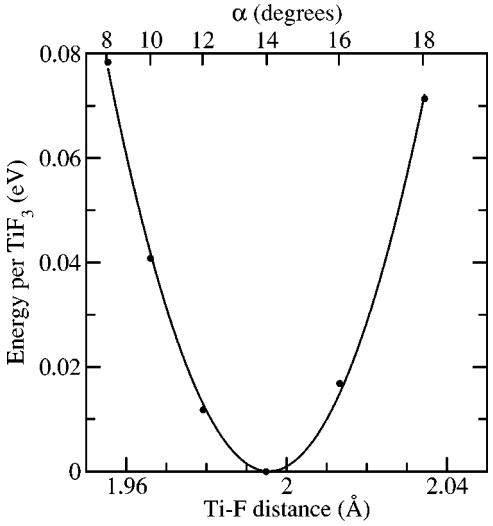

FIG. 6. LDA+U calculations for the antiferromagnetic low-T phase as a function of the tilt angle and fixed volume V_m and $c/a=1.0315$ ratio. The optimal angle is 14.1°, which corresponds to a Ti-F distance of 1.996 Å. The spring constant is 15.95 eV/Å^2.

nonmagnetic calculations give $U_1^{eff}=U-J/2=7.66$ eV. From the fully polarized magnetic calculation, the quadratic energy, and linear $\mu_{1/2}$ fit we find $U_2^{eff}=U-J=7.24$ eV, such that $U=8.08$ eV and $J=0.84$ eV. The Hund coupling parameter J should be compared with the spin-up and -down energy band splitting in ferromagnetic LDA calculations (Fig. 3), which is $J=0.87$ eV.

V. LDA+U RESULTS

The volume optimization of the high-symmetry phase gives $V_0=61.8$ Å^3 using two formula units per unit cell with $R3c$ point group symmetry operations and fixed $\phi=0°$ and $c/a=1$. The bulk modulus extracted from the Murnaghan fit shown in Fig. 5 is 110 GPa. The electron correlations on the Ti d orbitals reduces the bandwidth $(4t/U)$, such that the kinetic energy variation with respect to the lattice constant is smaller in the LDA+U functional, resulting in a larger equilibrium lattice constant compared to the LDA result.

The low-symmetry optimization was first done with respect to volume for a fixed experimental tilt angle $\phi=12°$ and the ratio $c/a=1.0316$. The optimal volume is 58.1 Å^3. Further optimization with respect to the tilt angle for the fixed equilibrium volume gives an additional energy gain of 130 K per Ti such that the distorted structure with the optimal tilt angle of 14° is lower in energy by 675 K per Ti. The parabola fit to the Ti-F bond length variation shown in Fig. 6 gives a spring constant $K=15.95$ eV/Å^2. The corresponding bulk modulus $B=K/(6V^{1/3})\approx 108$ GPa is an in excellent agreement with the Murnaghan fit of Fig. 5.

The density of states for the distorted structure is shown in Fig. 7. The fluorine $2p$ states are not much affected by the correlations, whereas dramatic differences are seen for the Ti d states. First, LDA+U predicts a gap for *both* high-T and low-T phases in the t_{2g} band, which is split into three distinct narrow peaks originating from the a_g and two e_g orbitals. The imposed rhombohedral symmetry of the supercell makes the lowest-energy a_g orbital pointing along the (111) direction to be fully occupied with a spin-up electron on one atom and a spin-down electron on the other atom coupled antiferromagnetically. The electronic properties of TiF_3 can be de-

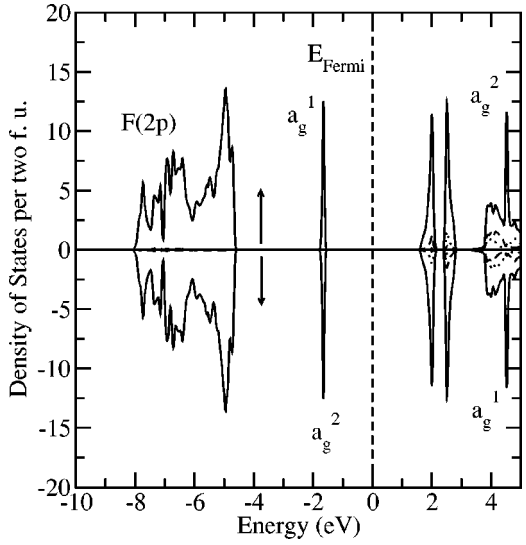

FIG. 7. Density of states per two formula units per eV. The two electrons in the unit cell fill the a_g^1 spin-up orbital on atom one and the a_g^2 spin-down orbital on the second atom peaked at -1.64 eV. The two lowest unoccupied peaks (at 2.01 eV and 2.52 eV) are due to the e_g orbitals of the t_{2g} manifold. The lower-energy orbital is due to the e_g orbital of the same atom and spin as the occupied a_g orbital. The broadbands 2 eV higher in energy shown by the dashed and dotted lines are due to the $e_g=\{x^2-y^2,3z^2-r^2\}$ orbitals split by crystal field. The empty a_g orbital with opposite spin at 4.53 eV forms a resonance in the crystal field e_g background.

scribed by the Hubbard Hamiltonian

$$\mathcal{H}_{\rm el} = \sum_{i,\alpha\beta,\sigma} -t(c^{\dagger}_{\alpha\beta,\sigma,i}c_{\alpha\beta,\sigma,i+\alpha} + c^{\dagger}_{\alpha\beta,\sigma,i}c_{\alpha\beta,\sigma,i+\beta}) + \sum_{i,\alpha\beta,\sigma} \frac{U}{2}(n_{\alpha\beta,\sigma,i}n_{\alpha\beta,-\sigma,i}) + \sum_{i,\alpha\beta\neq\alpha'\beta',\sigma,\sigma'} \frac{U' - J\delta_{\sigma,\sigma'}}{2}(n_{\alpha\beta,\sigma,i}n_{\alpha\beta,\sigma',i}). \quad (4)$$

The first term is a kinetic energy term described in Sec. III. To place two electrons with opposite spins costs energy U, if they occupy the same orbital, or U', if they are on different orbitals. If the spins of two electrons on different orbitals are aligned, the energy cost is reduced by J. In the atomic limit the relation $U = U' + 2J$ holds. Then the splitting between the a_g and e_g orbitals for a single-site Hubburd model would be $U' - J \approx 5.6$ eV. The atomic limit value of splitting is larger from the complete LDA+U solution ≈ 4 eV (see Fig. 7) where only a fraction of d electrons inside the muffin-tin sphere experiences the LDA+U potential. The second-order perturbation theory of the Hamiltonian [Eq. (4)] with respect to t/U predicts an insulating antiferromagnetic ground-state solution for parameters $U = 8.1$ eV, $J = 0.9$ eV, and $t = 0.22$ eV.

The superexchange energies per Ti of the antiferromagnetic Néel state and ferromagnetic solutions, with the a_g orbital [Eq. (2)] occupied in both cases, are

$$E_{\rm AFM} = -\frac{4t^2}{3}\frac{1}{U'} - \frac{8t^2}{3}\frac{1}{U},$$

$$E_{\rm FM} = -\frac{4t^2}{3}\frac{1}{U' - J}, \quad (5)$$

where the first term is due to virtual hopping of the localized electron on the six neighboring e_g orbitals. The second term in $E_{\rm AFM}$ is due to virtual hopping of the a_g orbital to the six neighbors with hopping amplitude $2t/3$, and it is missing in the ferromagnetic ground state due to the Pauli principle. The LDA+U energy differences between the ferromagnetic and antiferromagnetic ground states and the fixed optimal distorted geometry are shown in Fig. 8. Both the perturbation theory and LDA+U results predict the antiferromagnetic to ferromagnetic transition at $U/J \approx 4$. For the large U/J values LDA+U underestimates the exchange energy by a factor of 2 and for the realistic parameter of $U = 8.1$ eV it predicts an energy difference of 72 K between the two phases. Neglecting the zero-point energy of the spin waves the energy difference between the parallel and antiparallel classical spins on a cubic lattice is $6JS(S+1)$ (Ref. 21). For spin $S = 1/2$ this yields $J = 16$ K and the corresponding Néel temperature in the mean-field approximation is $T_{\rm N} = 1.5J = 24$ K. The quantum fluctuations reduce the Néel temperature to $T_{\rm N} = 0.946J = 15$ K (Ref. 22). However, a neutron diffraction experiment[23] did not reveal any long-range magnetic order down to 10 K. Whether the absence of magnetic long-range order in TiF_3 is an intrinsic effect due to the coupling of the orbital and spin degrees of freedom or extrinsic due to the presence of the multidomain structure observed in the low-symmetry phase by Mogus-Milankovic *et al.*[3] requires further theoretical and experimental investigations.

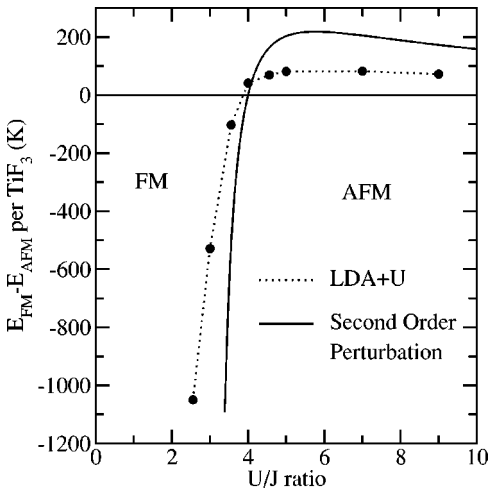

FIG. 8. Energy difference of the total energy of ferromagnetic and antiferromagnetic solutions as a function of U/J ratio. The solid line is a second-order perturbation theory for the fixed values $J = 0.9$ eV and $t = 0.225$ eV. The dots are LDA+U results with fixed $J = 0.9$ eV and optimal low-temperature geometry.

VI. PRESSURE ANOMALY

X-ray diffraction measurements under pressure by Sowa and Ahsbahs[24] allow us to determine the experimental bulk modulus of TiF_3. Figure 9(a) shows data points along with a Birch-Murnaghan equation-of-state fit. The fit to the full

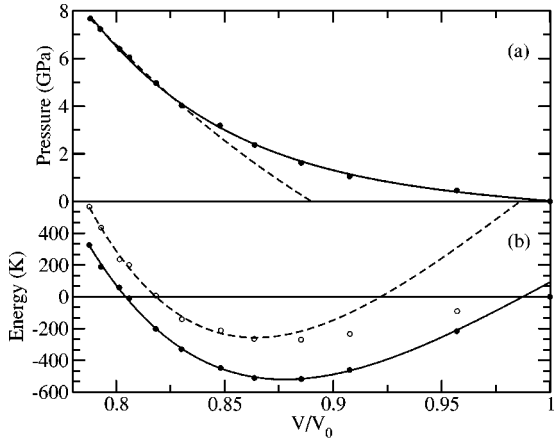

FIG. 9. (a) Experimental P-V diagram fitted by the Birch-Murnaghan equation of state to all data points (solid line) and the first six high-pressure points (dashed line). (b) Bulk modulus calculations using the cell parameters given in Table I. Energies of LDA (LDA+U) calculations are shown by open (solid) circles. The Birch-Murnaghan fit to the high-pressure points is shown by the dashed (solid) line for LDA (LDA+U) calculations. The zero energy is chosen at the ambient pressure value.

TABLE I. The unit cell parameters for the bulk modulus calculations. The normalized volume V/V_0 and c/a ratios are taken from Sowa and Ahsbahs (Ref. 24). For LDA+U calculations we used experimental volume $V_0=58.3$ Å^3 at ambient pressure (Ref. 24) and we choose a smaller $V_0=56.2$ Å^3 for LDA calculations to match the LDA optimal value. For given volume and c/a ratios the tilt angle was chosen such that Ti-F bond length, Eq. (1), is constant and equal to $d_{Ti\text{-}F}=1.947$ Å and $d_{Ti\text{-}F}=1.996$ Å for LDA and LDA+U, respectively.

p (GPa)	V/V_0	c/a	$\phi°$ LDA	$\phi°$ LDA+U
0.0001	1.000	1.023	10.4	13.9
0.46	0.957	1.056	14.3	17.0
1.05	0.908	1.099	17.9	20.2
1.62	0.885	1.118	19.4	21.5
2.37	0.864	1.138	20.8	22.8
3.18	0.848	1.155	21.7	23.6
4.03	0.830	1.167	22.8	24.6
4.97	0.818	1.181	23.5	25.3
6.05	0.806	1.187	24.2	25.9
6.40	0.801	1.189	24.4	26.2
7.23	0.793	1.193	24.9	26.6
7.67	0.788	1.198	25.2	26.9

range of pressures predicts a physically an unreasonable small bulk modulus $B=7.5$ GPa and an unphysically large coefficient $K_2=142$ GPa^{-1}. The first derivative is fixed to $K_1=4$ in the Birch-Murnaghan equation of state:

$$P(V)=3Bf(1+2f)^{5/2}\left[1+\frac{3f^2}{2}\left(BK_2+\frac{35}{9}\right)\right], \qquad (6)$$

where $f=0.5[(V_0/V)^{2/3}-1]$ and V_0 is the volume at ambient pressure. The high-pressure points (above 4 GPa) can be fitted by Eq. (6) to give $B=51$ GPa and a normal $K_2=-0.005$ GPa^{-1}. However, the volume at normal pressure has to be fixed to $V_0=51.9$ Å^3, which is 11% smaller than the observed one.

In the present work we calculate the bulk modulus of the lower-symmetry phase using the experimental c/a and V/V_0 ratios.[24] The tilt angle was chosen to keep the Ti-F bond length, Eq. (1), constant for all pressure values. We fix $d_{Ti\text{-}F}=1.947$ Å and $d_{Ti\text{-}F}=1.996$ Å for LDA and LDA+U calculations, respectively. For LDA+U calculations V_0 was fixed to the experimental value[24] $V_0=58.3$ Å^3, while for the LDA it is reduced to match the optimal volume $V_0=56.2$ Å^3 to eliminate strain effects. The results of calculations for the unit cell parameters given in Table I are shown in Fig. 9(b). The high-pressure points can be fitted by Eq. (6) to give a bulk modulus of $B=42$ GPa for LDA and $B=29$ GPa for LDA+U functionals with corresponding coefficients $K_2=-0.011$ GPa^{-1} and $K_2=-0.008$ GPa^{-1} and optimal volumes $V/V_0=0.86$ and $V/V_0=0.88$, which are in agreement with the ambient pressure volume deduced from the high-pressure experimental data. The energies in the global minimums in LDA and LDA+U calculations are 270 K and 525 K per TiF_3 lower than that of the experimentally observed structural parameters. A shallower minimum in the LDA can be explained by the kinetic energy loss due to the octahedron tilting. In LDA+U the kinetic energy is suppressed due to correlations and does not change much with tilting.

We speculate that this anomalous behavior of the compressibility of TiF_3 may be due to the presence of domain walls in the low-symmetry phase observed in Ref. 3. Under applied pressure the crystal becomes a single domain. An alternative explanation is the phonon contribution to the free energy which in principle depends on pressure. Additional calculations of the phonon spectrum and Gruneisen parameter are needed to estimate the phonon contribution to the bulk modulus anomaly.

VII. CONCLUSION

We used density-functional theory to predict the electronic and magnetic properties of TiF_3. The LDA predicts TiF_3 to be a ferromagnetic metal with a fully saturated moment $1\mu_B$ per Ti. The energies of the high- and low-symmetry structures are degenerate, such that the pure electron-phonon and electrostatic (Madelung) model does not explain the observed phase transition at $T_c=370$ K. The correlations are essential to suppress the kinetic energy loss of Ti t_{2g} electrons to favor the distortions. To model electron correlations on Ti d orbitals we use the LDA+U approach, which requires the input parameters U and J. We determine these parameters by calculating electron correlations on the TiF_6^{2-} ion and find $U=8.1$ eV and $J=0.9$ eV. LDA+U predicts TiF_3 to be an antiferromagnetic insulator with spin 1/2 per Ti. We find a long-range order of Ti a_g orbitals with a wave vector (000). The low-temperature phase is lower in energy by about 900 K per TiF_3 in LDA+U calculations, which suggests that electron-electron correlations are important.

Using the experimentally determined c/a and V/V_0 ratios we find a global minimum at 14% (LDA) and 12% (LDA+U) volumes smaller than the observed ambient pressure volume, which are consistent with the ambient pressure volume deduced from the experimental high-pressure data. The experimentally observed larger volume at the ambient pressure and the unusual behavior of the bulk modulus could be understood once the phonon contribution to the free energy is included. The zero phonon energy is in principle pressure dependent and can alter the position of the energy global minimum and the bulk modulus. The Gruneisen parameter calculations and experimental studies of the phonon spectrum under pressure will help to elucidate this problem.

ACKNOWLEDGMENTS

We are grateful to Fabian Essler for many valuable discussions, Warren Pickett for help in LDA+U calculations, and Dick Watson for useful suggestions. The computations were performed on the BNL galaxy cluster. This work was supported in part by DOE Grant No. DE-AC-02-98CH10886.

*Present address: IBM Research Division, T.J. Watson Research Center, Yorktown Heights, NY 10598.

[1] D.G. Isaak, R.E. Cohen, M.J. Mehl, and D.J. Singh, Phys. Rev. B **47**, 7720 (1993).

[2] M. Mochizuki and M. Imada, J. Phys. Soc. Jpn. **70**, 2872 (2001).

[3] A. Mogus-Milankovic, J. Ravez, J.P. Chaminade, and P. Hagenmuller, Mater. Res. Bull. **20**, 9 (1985).

[4] B.J. Kennedy and T. Vogt, Mater. Res. Bull. **37**, 77 (2002).

[5] J. Ravez, A. Mogus-Milankovic, and J.P. Chaminade, Mater. Res. Bull. **20**, 9 (1985).

[6] P. Daniel, A. Bulou, M. Rousseau, J.L. Fourquet, J. Nouet, M. Leblanc, and R. Burriel, J. Phys.: Condens. Matter **2**, 5663 (1990); P. Daniel, A. Bulou, M. Rousseau, J. Nouet, and M. Leblanc, Phys. Rev. B **42**, 10 545 (1990).

[7] P.B. Allen, Y.R. Chen, S. Chaudhuri, and C.P. Grey, cond-mat/0311014 (unpublished).

[8] Y.R. Chen, P.B. Allen, and V. Perebeinos, Phys. Rev. B **69**, 054109 (2004).

[9] V.I. Anisimov and O. Gunnarsson, Phys. Rev. B **43**, 7570 (1991); V.I. Anisimov, J. Zaanen, and O.K. Andersen, *ibid.* **44**, 943 (1991).

[10] M.R. Pederson and K.A. Jackson, Phys. Rev. B **41**, 7453 (1990); K.A. Jackson and M.R. Pederson, *ibid.* **42**, 3276 (1990); M.R. Pederson and K.A. Jackson, *ibid.* **43**, 7312 (1991); D.V. Porezag and M.R. Pederson, *ibid.* **54**, 7830 (1996); A. Briley, M.R. Pederson, K.A. Jackson, D.C. Patton, and D.V. Porezag, *ibid.* **58**, 1786 (1998).

[11] I. Solovyev, N. Hamada, and K. Terakura, Phys. Rev. B **53**, 7158 (1996).

[12] W.E. Pickett, S.C. Erwin, and E.C. Ethridge, Phys. Rev. B **58**, 1201 (1998).

[13] I.V. Solovyev and K. Terakura, in *Electronic Structure and Magnetism of Complex Materials*, edited by D. J. Singh and D. A. Papaconstantopoulos (Springer, Berlin, 2003).

[14] D.J. Singh, *Planewaves, Pseudopotentials and the LAPW Method* (Kluwer Academic, Boston, 1994).

[15] D.J. Singh, Phys. Rev. B **43**, 6388 (1991).

[16] P. Blaha, K. Schwarz, G.K.H. Madsen, D. Kvasnicka, and J. Luitz, *WIEN2K, An Augmented Plane Wave Plus Local Orbitals Program For Calculating Crystal Properties* (Vienna University of Technology, Austria, 2001).

[17] J.P. Perdew and Y. Wang, Phys. Rev. B **45**, 13 244 (1992).

[18] F.D. Murnaghan, Am. J. Math. **49**, 235 (1937).

[19] V.I. Anisimov, I.V. Solovyev, M.A. Korotin, M.T. Czyzyk, and G.A. Sawatzky, Phys. Rev. B **48**, 16 929 (1993); I.V. Solovyev, P.H. Dederichs, and V.I. Anisimov, *ibid.* **50**, 16 861 (1994); A.I. Liechtenstein, V.I. Anisimov, and J. Zaanen, *ibid.* **52**, 5467 (1995); A.B. Shick, A.I. Liechtenstein, and W.E. Pickett, *ibid.* **60**, 10 763 (1999).

[20] J.C. Slater and G.F. Koster, Phys. Rev. **94**, 1498 (1954).

[21] P.W. Anderson, Phys. Rev. **86**, 694 (1952).

[22] A.W. Sandvik, Phys. Rev. Lett. **80**, 5196 (1998).

[23] T. Vogt *et al.* (unpublished).

[24] H. Sowa and H. Ahsbahs, Acta Crystallogr., Sect. B: Struct. Sci. **54**, 578 (1998).